Regulation of the Epithelial Na+ Channel by the Protein Kinase CK2*⸋

Tanja Bachhuber[‡1], Joana Almaça[‡§1,2], Fadi Aldehni[‡], Anil Mehta[¶], Margarida D. Amaral[¶‖], Rainer Schreiber[‡], and Karl Kunzelmann[‡3]

From the ‡Institut für Physiologie, Universität Regensburg, Universitätsstraβe 31, D-93053 Regensburg, Germany, the ¶Department of Maternal and Child Health Sciences, University of Dundee, Ninewells Hospital, Dundee DD1 9SY, United Kingdom, the §Faculdade de Ciências, Universidade de Lisboa, 1749-016 Lisboa, Portugal, and the ‖Centre of Human Genetics, National Institute of Health, 1649-016 Lisboa, Portugal

CK2 is a ubiquitous, pleiotropic, and constitutively active Ser/Thr protein kinase that controls protein expression, cell signaling, and ion channel activity. Phosphorylation sites for CK2 are located in the C terminus of both β- and γ-subunits of the epithelial Na+ channel (ENaC). We examined the role of CK2 on the regulation of both endogenous ENaC in native murine epithelia and in *Xenopus* oocytes expressing rENaC. In Ussing chamber experiments with mouse airways, colon, and cultured M1-collecting duct cells, amiloride-sensitive Na+ transport was inhibited dose-dependently by the selective CK2 inhibitor 4,5,6,7-tetrabromobenzotriazole (TBB). In oocytes, ENaC currents were also inhibited by TBB and by the structurally unrelated inhibitors heparin and poly(E:Y). Expression of a trimeric channel lacking both CK2 sites ($\alpha\beta_{S631A}\gamma_{T599A}$) produced a largely attenuated amiloride-sensitive whole cell conductance and rendered the mutant channel insensitive to CK2. In *Xenopus* oocytes, CK2 was translocated to the cell membrane upon expression of wt-ENaC but not of $\alpha\beta_{S631A}\gamma_{T599A}$-ENaC. Phosphorylation by CK2 is essential for ENaC activation, and to a lesser degree, it also controls membrane expression of $\alpha\beta\gamma$-ENaC. Channels lacking the Nedd4-2 binding motif in β-ENaC (R561X, Y618A) no longer required the CK2 site for channel activity and siRNA-knockdown of Nedd4-2 eliminated the effects of TBB. This implies a role for CK2 in inhibiting the Nedd4-2 pathway. We propose that the C terminus of β-ENaC is targeted by this essential, conserved pleiotropic kinase that directs its constitutive activity toward many cellular protein complexes.

Electrogenic Na+ absorption across the apical membrane of epithelia utilizes an amiloride-sensitive channel (ENaC)[4] composed of three ($\alpha\beta\gamma$) subunits produced from different genes (6). In kidney-collecting duct, distal colon, airway, secretory ducts from a variety of organs, and the absorptive sweat duct, ENaC is regulated by an interaction between the β- and γ-subunits (at their C terminus) and the E3-ubiquitin ligase Nedd4-2. The WW domains of Nedd4-2 bind proline-rich PY (P*XX*Y) motifs in each ENaC subunit leading to channel ubiquitination, internalization, and degradation and hence channel inactivation (7, 17). Nedd4-2 interaction with ENaC is positively and negatively controlled by phosphorylation of either Nedd4-2, or the C termini of both β- and γ-ENaC. Accordingly, the aldosterone-induced serum and glucocorticoid-dependent kinase, Sgk-1, phosphorylates Nedd4-2 on serines (Ser) 444 and 338, thereby reducing its interaction with the channel and causing enhanced ENaC activity (7, 23). Apart from this, Sgk-1 also phosphorylates α-ENaC directly at Ser-621, causing a stimulatory effect on the channel, which appears to be Nedd-4-2-independent (8). Protein kinase A (PKA), which is known to activate ENaC in alveolar epithelial cells, sweat duct, and kidney, was also shown to phosphorylate Nedd4-2 (at serine residues 221, 246, and 327) and to reduce binding to ENaC (22). Moreover, PKA prevents inhibition of ENaC by preventing β-ENaC phosphorylation at threonine (Thr) 613 by the extracellular-regulated kinase (Erk) (26). Indeed, phosphorylation of Thr-613 in β-ENaC and Thr-623 in γ-ENaC were previously shown to increase channel affinity toward Nedd4-2, thereby down-regulating channel activity (20).

Thus, differential phosphorylation of both β- and γ-ENaC subunits can either enhance or reduce its affinity for Nedd4-2, thereby controlling its degradation and hence the channel activity. Along this line, the G protein-coupled receptor kinase 2 (Grk2) was found recently to upregulate the activity of ENaC in salivary duct cells (9). Grk2 acts at the C terminus of β-ENaC phosphorylating Ser-633, *i.e.* twenty amino acids downstream of Erk. Grk2 increases the activity of ENaC by rendering the channel insensitive to Nedd4-2 (9). Notably, an increased Grk2 activity has been reported to be associated with hypertension in humans and in animal models (11). Therefore, imbalance in ENaC channel regulation by activatory or inhibitory pathways may lead to inappropriate Na+ absorption, hypertension, or cystic fibrosis (15).

⸋ The on-line version of this article (available at http://www.jbc.org) contains supplemental Fig. S1.
[1] Both authors contributed equally to the present work.
[2] Recipient of the SFRH/BD/29134/2006 PhD fellowship from FCT (Portugal).
[3] To whom correspondence should be addressed. Tel.: 49-0-941-943-4302; Fax: 49-0-941-943-4315; E-mail: uqkkunze@mailbox.uq.edu.au.
[4] The abbreviations used are: ENaC, epithelial Na+ channel; ERK, extracellular signal-regulated kinase; CK, casein kinase; BSA, bovine serum albumin; PBS, phosphate-buffered saline; wt, wild type; TBB, 4,5,6,7-tetrabromobenzotriazole; DMAT, 2-dimethylamino-4,5,6,7-tetrabromo-1*H*-benzimidazole; Grk2, G protein-coupled receptor kinase 2; siRNA, small interfering RNA.

Additional phosphorylation sites at the C terminus of the β- and γ-subunits of ENaC include those for the pleiotropic but essential protein casein kinase 2 (CK2) (21). It has been demonstrated that CK2 specifically binds to and phosphorylates the C termini of both these ENaC subunits. As found for the Grk2 site (Ser-633) in β-ENaC, a pair of CK2 phosphorylation sites (βSer-631 and γThr-599) are located in close proximity to their respective PY motifs. CK2 is not easy to study, as siRNA approaches invariably impact on a number of targets in multiple pathways, some of which coupled to its essential function for cell survival. In a previous study, no contribution of CK2 to regulation of ENaC was observed following the mutation of single putative CK2 sites (21). Notwithstanding, we investigated a role for CK2 on ENaC function in native epithelia from airway and colon as well as in *Xenopus* oocytes expressing rat ENaC. We found that constitutive CK2 phosphorylation not only maintains ENaC active, but it also controls the membrane expression of its subunits.

MATERIALS AND METHODS

Ussing Chamber Experiments—Tracheas and distal colon were removed from mice euthanized by ethically approved institutional procedures (C57BL/6, Charles Rivers, Germany). Tissues were put immediately into ice-cold buffer solution of the following composition (mmol/liter): NaCl 145, KCI 3.8, D-glucose 5, MgCI$_2$ 1, HEPES 5, Ca^{2+} gluconate 1.3. After stripping the colonic mucosa and opening tracheas by a longitudinal cut, tissues were mounted into a micro Ussing chamber with a circular aperture of 0.95 mm^2. Mouse M-1 kidney cortex-collecting duct cells (kindly provided by C. Korbmacher, Physiologisches Institut, Universität Erlangen, Germany) were grown to confluence on permeable supports and mounted into the Ussing chamber (2). Luminal and basolateral sides of the epithelium were perfused continuously at a rate of 5 ml/min. The bath solution containing (mmol/liter) NaCl 145, KH$_2$PO$_4$ 0.4, K$_2$HPO$_4$ 1.6, D-glucose 5, MgCI$_2$ 1, HEPES 5, and calcium gluconate 1.3, was heated to 37 °C, and the pH was adjusted to 7.4. Experiments were carried out under open circuit conditions. Values for transepithelial voltages (V$_{te}$) were referred to the serosal side of the epithelium. Transepithelial resistance (R$_{te}$) was determined by applying short (1 s) current pulses ($\Delta l = 0.5$ μA) and after subtracting the resistance of the empty chamber, using Ohm's law (R$_{te}$ = $\Delta V_{te}/\Delta I$). Transepithelial resistances were 63 $\pm$ 3.8 Ωcm^2; n = 12 (trachea), 31 $\pm$ 2.1; n = 13 (colon), and 669 $\pm$ 45 Ωcm^2; n = 38 (M1).

cRNAs for ENaC Subunits and CFTR—cDNAs-encoding rat (FLAG-tagged or non-tagged) $\alpha\beta\gamma$-ENaC (kindly provided by Prof. Dr. B. Rossier, Pharmacological Institute of Lausanne, Switzerland, Ref. 12) and the Cl$^-$ channels CFTR were linearized in pBluescript with Notl or Mlul, and *in vitro* transcribed using T7, T3, or SP6 promotor and polymerase (Promega). Isolation and microinjection of oocytes have been described in detail elsewhere (2). The ENaC mutants β_{S631A}, γ_{T599A}, β_{R561X}, β_{Y618A}, and β_{S633A} were generated by PCR, and correct sequences were verified by sequencing.

Double Electrode Voltage Clamp—Oocytes were injected with cRNA (10 ng, 47 nl double-distilled water). Water-injected oocytes served as controls. 2–4 days after injection, oocytes were impaled with two electrodes (Clark Instruments Ltd, Salisbury, UK), which had a resistance of <1 MΩ when filled with 2.7 mol/liter KCI. Using two bath electrodes and a virtual ground head stage, the voltage drop across R$_{serial}$ was effectively zero. Membrane currents were measured by voltage clamping (oocyte clamp amplifier, Warner Instruments LLC, Hamden CT) in intervals from -90 to $+30$ mV, in steps of 10 mV, each 1 s. The bath was continuously perfused at a rate of 5 ml/min. All experiments were conducted at room temperature (22 °C).

Chemiluminescence Measurements—Oocytes were fixed for 60 min at room temperature with 3% paraformaldehyde (in Tris-buffered saline (TBS), pH 8.0) and washed with TBS; (mM) 50 Tris, 138 NaCl, 2.7 KCl, pH 8.0 at room temperature. Then oocytes were incubated for 60 min in TBS with 1% (w/v) bovine serum albumin (BSA), another 60 min with 1 μg/ml mouse monoclonal anti-FLAG M2 antibody in 1% BSA/TBS at 4 °C (Sigma-Aldrich), washed at 4 °C with 1% BSA/TBS and incubated with sheep anti-mouse IgG peroxidase-linked whole antibody (Amersham Biosciences) diluted 1:20,000 in 1% BSA/TBS for 40 min at 4 °C. Afterward oocytes were washed for 60 min at 4 °C in 1% BSA/TBS and finally in TBS (60 min, 4 °C). Oocytes were placed separately in 50 μl of ECL Plus Western blotting detection reagents (Amersham Biosciences). After incubation for 5 min at room temperature, chemiluminescence was measured in a BioOrbit 1250 Luminometer (Turku, Finland), and an integration period of 1 s was allowed.

Oocyte Staining—Oocytes were incubated for 60 min in ND96 solution (in mM: 96 NaCl, 2.0 KCl, 1.8 CaCl$_2$, 1.0 MgCl$_2$, 5.0 HEPES, pH 7.4), fixed for 60 min with 3% paraformaldehyde (in TBS, pH 8.0) and washed in TBS. After embedding in optimum cutting temperature compound (Sakura Finetek Europe, Zoeterwoude, NL), oocytes were cut to 20-μm slices with a cryostat (Leica CM3050 S, Wetzlar, Germany). Sections were put in either TBS or phosphate-buffered saline (PBS; (mM) 137 NaCl, 1.8 KH$_2$PO$_4$, 10.3 Na$_2$HPO$_4$, pH 7.4), incubated for 5 min in 0.1% (w/v) SDS in PBS and washed two times with either TBS or PBS. Sections were incubated for 60 min in TBS or PBS (5% BSA) and for 60 min at 37 °C with the anti-FLAG M2 antibody diluted 1:50 in 2% BSA/TBS or a goat polyclonal casein kinase IIα antibody (Santa Cruz Biotechnology, Heidelberg, Germany) diluted 1:25 in 2% BSA/PBS. Afterward sections were washed twice in PBS and incubated for 1 h with secondary antibodies (donkey anti-mouse IgG-Alexa Fluor 488 conjugated and donkey anti-goat IgG-Alexa Fluor 546 conjugated; Molecular Probes, Eugene, OR) at a dilution of 1:1000 in 2% BSA/PBS. Sections were washed two times with PBS for 5 min and covered with DakoCytomation fluorescent mounting medium (DakoCytomation, Inc., Carpinteria, CA). Images were obtained using a Zeiss Axiovert 200 m microscope with a $\times$63 objective (Carl Zeiss, Inc., Jena, Germany).

Materials and Statistical Analysis—All compounds used were of highest available grade of purity. Amiloride, 2-dimethylamino-4,5,6,7-tetrabromo-1*H*-benzimidazole (DMAT), forskolin, IBMX (3-isobutyl-1-methylxanthine), heparin, okadaic acid, poly(E:Y) peptide, and poly(K) were from Sigma. TBB was a generous gift from Prof. L. Pinna (Department of Biological Chemistry, University of Padua, Italy). The Nedd4-2 antibody was a generous gift from Prof. Dr. J. Loffing (University of Zür-
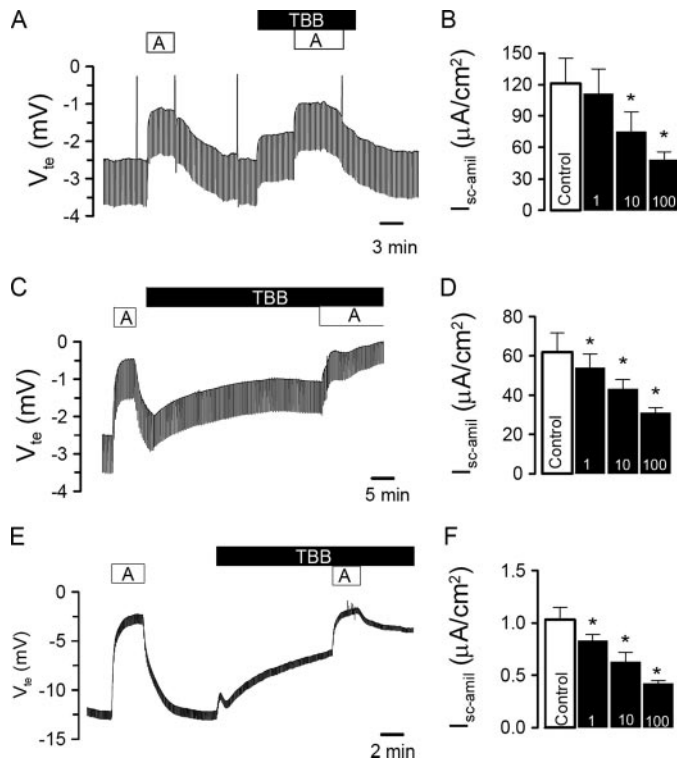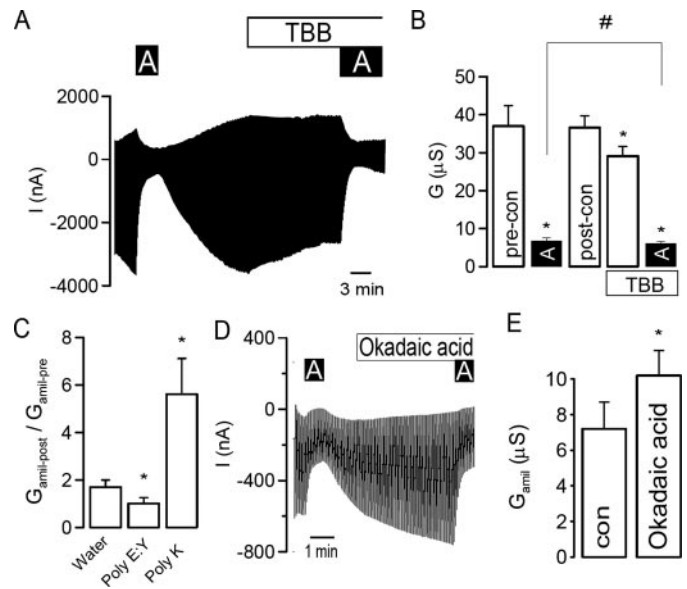
FIGURE 1. **CK2 activates ENaC in native epithelia and in epithelial cells.** Original Ussing chamber recordings of the transepithelial voltages V_{te} detected in mouse trachea (*A*), mouse colon (*C*), and M1 cells (*E*). Effects of amiloride (*A*, 10 μM) and the CK2 inhibitor TBB (10 μM). Concentration-dependence of the effects of TBB on amiloride-sensitive transport in trachea (*B*), colon (*D*), and M1 cells (*F*). The *asterisk* (*) indicates significant effects of TBB (paired *t*-tests, number of experiments: 9–13 for each series).

FIGURE 2. **CK2 activates ENaC in Xenopus oocytes.** *A*, current recording from a *Xenopus* oocyte expressing $\alpha\beta\gamma$-ENaC and effects of amiloride (10 μM) and TBB (10 μM). Oocytes were voltage-clamped from -90 mV to $+10$ mV in steps of 10 mV, and the resulting currents were recorded. *B*, summary of the effects of amiloride and TBB on whole cell conductance in ENaC-expressing oocytes. *C*, summary of the change of amiloride-sensitive conductance (G_{amil}) after injection of water, the CK2 inhibitor poly(E:Y) (50 μM) and CK2 activator poly(K) (50 μM), respectively. *D*, current recording of an ENaC-expressing oocyte and the effects of amiloride (*A*, 10 μM) and okadaic acid (100 nM). *E*, summary of the effect of okadaic acid on the amiloride-sensitive whole cell conductance measured in oocytes. The *asterisk* (*) indicates significant effects (paired *t*-test). The *number sign* (#) indicates a significant difference for the effects of amiloride before and after incubation with TBB (paired *t*-test, 6–25 experiments for each series).

ich, Switzerland). mNedd4-2-RNAi (5′-CCA UUU GUC CUA UUU CAC CUU CAU U-3′), xNedd4-2-RNAi (5′-GCG UGC CUA UGA AUG GAU U-3′), and mCK2-RNAi (5′-UUG UCA AGA AGA UCU AGG GCC UCC G-3′) were from Invitrogen (Paisley, UK). Scrambled RNA is a mixture of double-stranded RNA sequences that has no match to any of the known *Xenopus* mRNA sequences. Student's *t* test was used for statistical analysis. A *p* value of <0.05 was regarded as significant.

RESULTS

CK2 Blocker Inhibits ENaC Activity—We examined the contribution of CK2 to the regulation of epithelial Na$^+$ channels in native epithelia from mouse trachea and colon. In Ussing chamber experiments, we explored CK2-selective concentrations of the specific inhibitor TBB, which was shown to have no effect on over 30 other kinases. TBB selectivity depends on its ability to bind an unusual hydrophobic ATP binding site that differs from the equivalent in conventional kinases. Electrogenic Na$^+$ transport in mouse trachea was assessed by inhibition of ENaC with amiloride (10 μM) (Fig. 1*A*). TBB (10 μM) reduced the transepithelial voltage V_{te} and attenuated amiloride-sensitive short-circuit currents ($I_{sc-amil}$) in a dose-dependent manner (Fig. 1, *A* and *B*). Similarly, TBB significantly blocked amiloride-sensitive Na$^+$ transport in mouse distal colon (Fig. 1, *C* and *D*). This effect could be reproduced in cultured mouse M1-collecting duct cells, grown on permeable supports (Fig. 1, *E* and *F*). These combined results suggest that

endogenous epithelial Na$^+$ channels expressed in epithelial tissues are maintained in an active state by constitutively active CK2.

To further confirm regulation of epithelial Na$^+$ channels by CK2, the three ($\alpha\beta\gamma$)-ENaC subunits were expressed in *Xenopus* oocytes and examined in double electrode voltage clamp experiments. As shown in the original recording in Fig. 2*A*, the simultaneous expression of the three ENaC subunits produced a large current, which was inhibited by amiloride (A, 10 μM). The CK2 structure is virtually identical in *Xenopus* compared with mammals. Thus, TBB (10 μM) also significantly reduced amiloride-sensitive whole cell currents and conductance (G_{amil}), respectively (Fig. 2, *A* and *B*) in oocytes. Another compound, DMAT, has recently been shown to inhibit CK2 with higher inhibitory potency, but it has limited efficacy *in vivo* due to its rapid turnover.[5] At 2 μM, we did not observe inhibition of ENaC currents by DMAT in *Xenopus* oocytes; however, 5 μM reduced amiloride-sensitive ENaC conductance significantly from 31.9 ± 6.8 to 25.7 ± 4.1 μS ($n = 5$). Regulation of ENaC by CK2 was further validated using the structurally unrelated peptide inhibitor of CK2, poly(E:Y) and conversely, by activating CK2 with polylysine (poly(K)) (16, 24). The peptides were injected into oocytes at final concentrations between 10 and 100 μM, and amiloride-sensitive Na$^+$ conductances were compared before and 1–5 h after injection. During these few hours, ENaC conductance increased, almost doubling initial values in

---

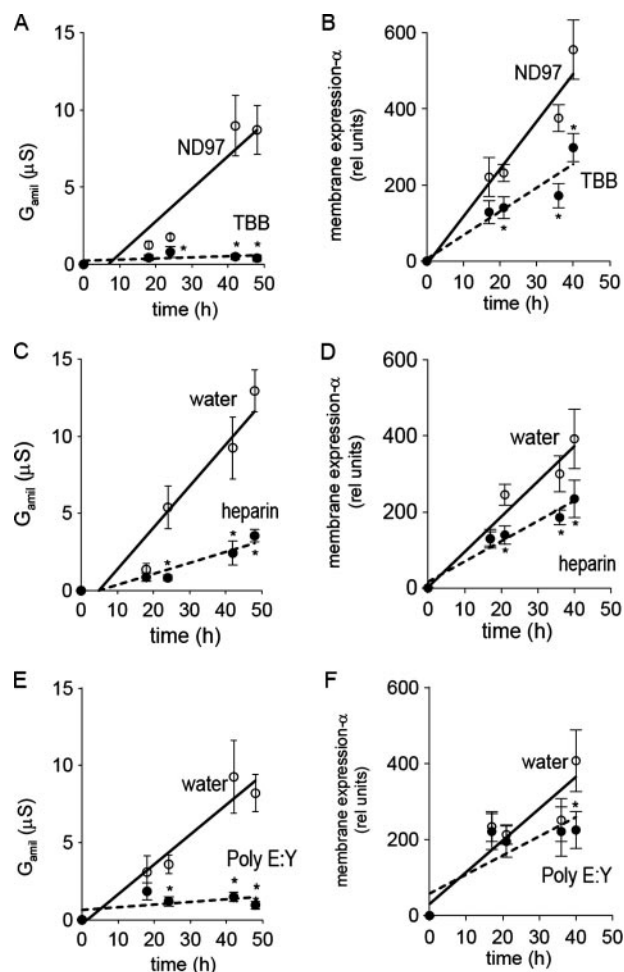[5] L. A. Pinna, personal communication.
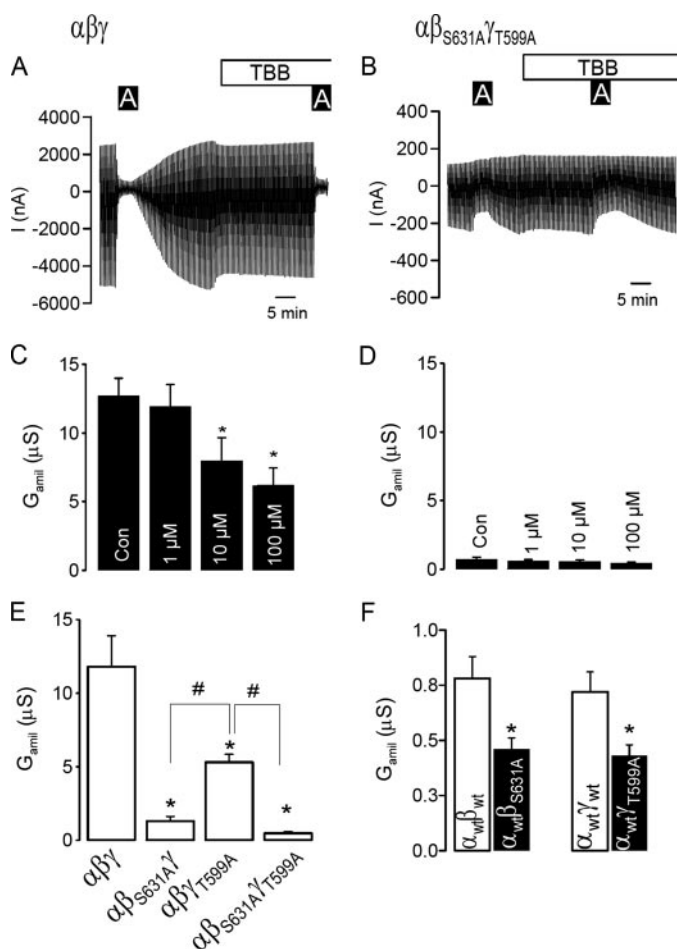
FIGURE 3. **Elimination of CK2 phosphorylation sites on ENaC inhibits channel activity.** *A*, current recording from a *Xenopus* oocyte expressing $\alpha\beta\gamma$-ENaC and effects of amiloride (10 μM) and TBB (10 μM). Oocytes were voltage-clamped from -90 mV to $+10$ mV in steps of 10 mV, and the resulting currents were recorded. *B*, current recording from a *Xenopus* oocyte expressing $\alpha\beta_{S631A}\gamma_{T559A}$-ENaC and effects of amiloride (10 μM) and TBB (10 μM). *C* and *D*, summaries of the effects of amiloride and TBB on G_{amil} generated by $\alpha\beta\gamma$-ENaC and $\alpha\beta_{S631A}\gamma_{T559A}$-ENaC. *E*, comparison of G_{amil} produced by wt-($\alpha\beta\gamma$)-, single mutants ($\alpha\beta_{S631A}\gamma$, $\alpha\beta\gamma_{T559A}$)-, and a double mutant ($\alpha\beta_{S631A}\gamma_{T559A}$)-ENaC. *F*, summaries of G_{amil} produced by dimeric wt-($\alpha\beta$, $\alpha\gamma$)- and mutant ($\alpha\beta_{S631A}$, $\alpha\gamma_{T559}$)-ENaC channels. The asterisk (*) and number sign (#) indicate a significant difference (paired t-test, 13–25 experiments for each series).

FIGURE 4. **CK2 controls membrane expression of ENaC in *Xenopus* oocytes.** Time course for G_{amil} (*A, C, E*) and membrane expression of α_{Flag}-ENaC (*B, D, F*). Oocytes were kept in ND97 or in ND97 containing TBB (10 μM), or were injected with heparin (10 μM), poly(E:Y) (50 μM), or equal amounts (30 nl) of water. The asterisk (*) indicates significant differences when compared with ND96 or water (unpaired t-tests, 6–13 experiments for each series).

water-injected controls (Fig. 2), This time-enhanced Na$^+$ conductance was nevertheless inhibited by poly(E:Y) and was further activated through stimulation of CK2 by poly(K) (Fig. 2*C*). CK2 is known to associate with protein phosphatase 2A (PP2A). To confirm phosphorylation-dependent activation of ENaC, oocytes were exposed to okadaic acid at a PP2A-specific concentration (10 nM), which further increased amiloride-sensitive Na$^+$ transport (Fig. 2, *D* and *E*). Thus ENaC appears to be stimulated by constitutively active CK2 with counter-regulation by PP2A-like inhibition. To further confirm this activation by CK2, injection of the nonspecific CK2 inhibitor heparin (10 μM) also reduced Na$^+$ conductance in *Xenopus* oocytes (Fig. 4*C*).

Removal of CK2 Sites from β- and γ-ENaC Inhibits Amiloride-sensitive Na$^+$ Conductance and Renders It Insensitive to TBB—Similar to endogenous Na$^+$ currents present in epithelial tissues (Fig. 1), ENaC expressed exogenously in *Xenopus* oocytes was inhibited by TBB in a dose-dependent manner (Fig. 3, *A* and *C*). ENaC contains two phosphorylation sites for CK2, in β-ENaC

(serine 631) and γ-ENaC (threonine 599). Changing both CK2 sites to alanines ($\alpha\beta_{S631A}\gamma_{T599A}$) virtually eliminated Na$^+$ conductance and rendered residual conductance of the double mutant channel insensitive to TBB (Fig. 3, *B* and *D*). Trimeric Na$^+$ channels carrying only one mutation in either β-ENaC ($\alpha\beta_{S631A}\gamma$) or γ-ENaC ($\alpha\beta\gamma_{T599A}$), produced more measurable but still significantly attenuated Na$^+$ conductances when compared with wt-ENaC (Fig. 3*E*). Moreover, the remaining amiloride-sensitive Na$^+$ conductances formed by dimeric $\alpha\beta$-ENaC and $\alpha\gamma$-ENaC channels were further reduced by β_{S631A} and γ_{T599A}, respectively (Fig. 3*F*). Finally, coexpression of hCK2 together with wt-ENaC increased G_{amil} (65.9 $\pm$ 9.0 μS; $n = 7$), when compared with injection of wt-ENaC alone (47.2 $\pm$ 8.1 μS; $n = 7$). Co-expression of hCK2 did not augment G_{amil} of $\alpha\beta_{S631A}\gamma_{T599A}$-ENaC (3.3 $\pm$ 0.7 μS; $n = 11$ *versus* 3.4 $\pm$ 0.5 μS; $n = 11$). Taken together, these results demonstrate that phosphorylation of β_{S631} and γ_{T599} is essential for ENaC.

CK2 Controls ENaC Activity and Membrane Expression of α-ENaC—To examine whether CK2 phosphorylation controls membrane expression of ENaC, FLAG-tagged α-ENaC was co-expressed with non-flagged $\beta\gamma$-ENaC in *Xenopus* oocytes. The
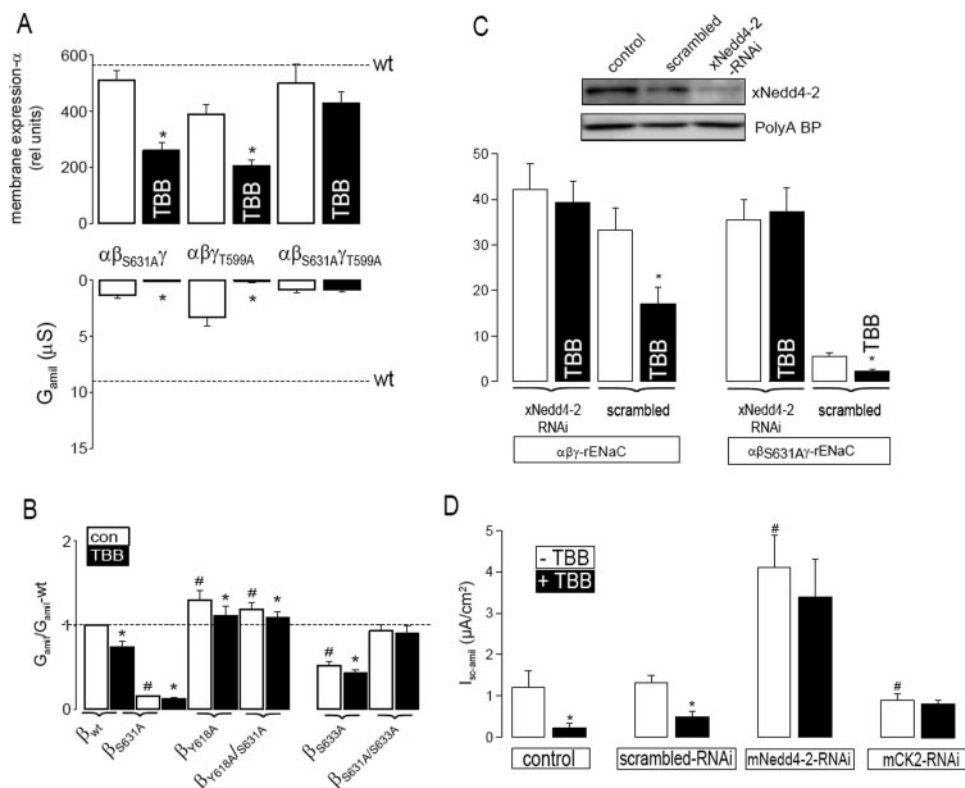
FIGURE 5. **CK2 is essential for ENaC activity and antagonizes the inhibitory effect of Nedd4-2 on ENaC.** *A*, summary of α-ENaC membrane expression and G_{amil} after 40 h. TBB inhibited membrane expression of α-ENaC via single mutants ($\alpha\beta_{S631A}\gamma$, $\alpha\beta\gamma_{T559A}$) but not that of the double mutant ($\alpha\beta_{S631A}\gamma_{T559A}$). G_{amil} was largely reduced for all mutants, and G_{amil} produced by the double mutant was no longer inhibited by TBB. *Dashed lines* indicate membrane expression and G_{amil} of wt-ENaC. *B*, whole cell conductances relative to wt-ENaC. A mutation in the PY motif (Y618A) of β-ENaC increased Na$^+$ conductance, and S631A no longer inhibited ENaC conductance. The Grk2 mutant S633A inhibited ENaC, but not as a double mutant S631A/S633A. *C*, inhibition of xNedd4-2 expression by siRNA-xNedd4-2 but not scrambled siRNA. The abundant poly(A)-binding protein indicates equal loading. Summary of ENaC whole cell conductances measured in the absence or presence of siRNA-xNedd4-2 or scrambled siRNA (see "Materials and Methods"). *D*, summary of the amiloride-sensitive short-circuit current and effects of TBB (10 μM) in control M1 cells and M1 cell treated with scrambled RNAi, mNedd4-2-RNAi, and mCK2-RNAi (see "Materials and Methods"). The *asterisk* (*) indicates significant effects of TBB (paired *t*-tests). The *number sign* (#) indicates a significant difference compared with control (unpaired *t*-test, 6–24 experiments for each series).

appearance of α_{Flag}-ENaC in the cell membrane was monitored by chemiluminescence, during an observation period of 40–48 h (Fig. 4, *B*, *D*, and *F* and Fig. 5*A*, see "Materials and Methods"). Control injection with non-flagged ENaC did not produce a chemiluminescence different from background (data not shown). In parallel, amiloride-sensitive Na$^+$ conductance was assessed at corresponding intervals (Fig. 4, *A*, *C*, and *E*). When $\alpha_{Flag}\beta\gamma$-ENaC was expressed in control oocytes, both G_{amil} and membrane expression continuously increased (Fig. 4, *A* and *B*). In contrast, when oocytes were kept in 10 μM TBB-containing buffer, amiloride-sensitive Na$^+$ conductance was completely abolished, and membrane expression was significantly reduced, albeit not completely. Moreover, co-injection of $\alpha\beta\gamma$-ENaC-cRNAs together with the CK2 inhibitors heparin (final concentration 10 μM) or the peptide inhibitor poly(E:Y) (final concentration 50 μM) also inhibited Na$^+$ conductance along with membrane expression of α-ENaC (Fig. 4, *C–F*). Finally, M1 cells were grown on permeable supports, in the absence or presence of 10 μM TBB. As observed in oocytes, TBB reduced amiloride-sensitive transport from 2.05 $\pm$ 0.35 μA/cm^2 (n = 19) to 1.52 $\pm$ 0.25 μA/cm^2 (n = 16). Thus, CK2 phosphorylation differen-

tially controls membrane expression of α-ENaC and ENaC activity. Of note, the inhibitory effect on conductance (3–5-fold) was significantly greater than on membrane expression (typically 2-fold).

CK2 Is Essential for ENaC Activity, but Has a Small Effect on Membrane Expression of α-ENaC—The contribution of both CK2 phosphorylation sites in β-ENaC and γ-ENaC, to membrane expression of α-ENaC was further examined by expressing single mutants ($\alpha_{Flag}\beta_{S631A}\gamma$-ENaC or $\alpha_{Flag}\beta\gamma_{T599A}$-ENaC) or the double mutant ($\alpha_{Flag}\beta_{S631A}\gamma_{T599A}$-ENaC) in oocytes. For the sake of simplicity, we only show a summary of the data obtained for membrane expression and ENaC conductance after 40 h of expression of those ENaC variants (relative to wild type). Importantly, single mutations in β-ENaC or γ-ENaC largely reduced the Na$^+$ conductance but had only a small effect on membrane expression. Elimination of both CK2 sites in β-ENaC and γ-ENaC also strongly reduced G_{amil}, with a minor effect on membrane expression (Fig. 5*A*). Of note, TBB reduced α-ENaC expression only when one CK2 site was intact.

The nearby located Grk2 phosphorylation site Ser-633 was reported to control Nedd4-2 binding to ENaC (9). We explored whether the same might hold true for CK2 phosphorylation sites. To this end, we compared whole cell conductances of several ENaC mutants to that of wt-ENaC. A mutation in the Nedd4-2 binding site (β_{Y618A}) increased ENaC whole cell conductance relative to the wild type and eliminated the inhibitory effect of S631A on ENaC conductance (Fig. 5*B*). This strongly suggests that CK2 phosphorylation at Ser-631 antagonizes the inhibitory action of Nedd4-2 in ENaC (20) (Fig. 8). Similarly, when we expressed the truncated $\alpha\beta_{R561X}\gamma$-ENaC channel, we found that amiloride-sensitive whole cell conductance was largely increased (64.5 $\pm$ 5.9 μS; n = 14) when compared with $\alpha\beta\gamma$-ENaC, and was now unaffected by 10 μM TBB (64.1 $\pm$ 6.1 μS). Interestingly, mutating the Grk2 site also reduced ENaC conductance; however, eliminating both CK2 and Grk2 sites in β-ENaC produced a channel with similar activity to that of wt-ENaC (Fig. 5*B*). This suggests that the closely located phosphorylation sites of CK2 and Grk2 (Ser-631, Ser-633) influence each other.

The role of Nedd4-2 on CK2 regulation of ENaC was further examined by siRNA-knockdown of xNedd4-2, similar to a recent study (Fig. 5*C*) (18). Two remarkable results were
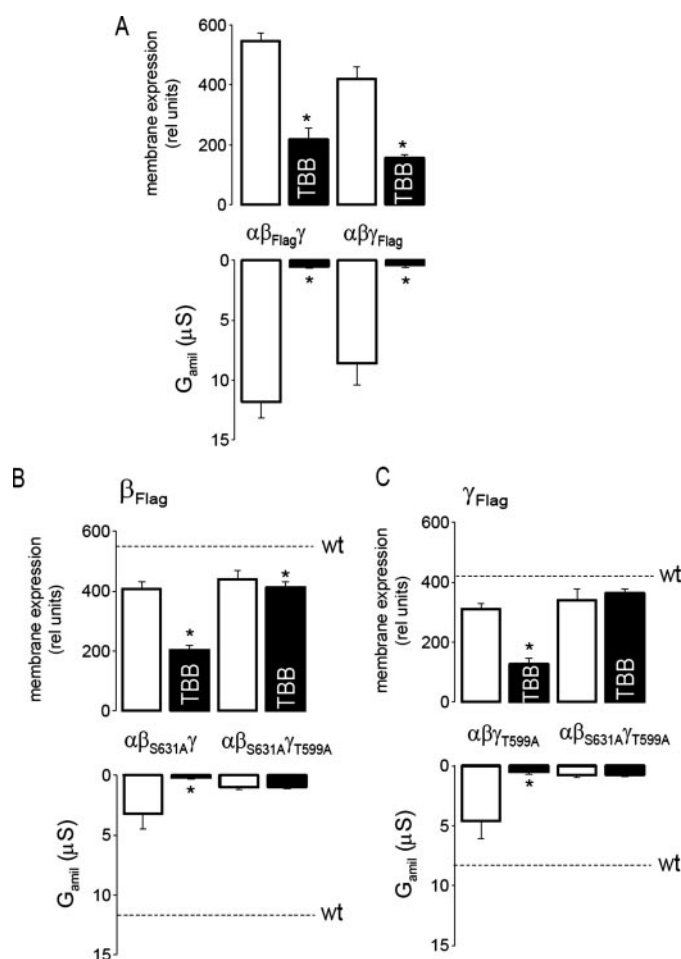
obtained, namely: (i) wt-ENaC was no longer inhibited by TBB. (ii) $\alpha\beta_{S631A}\gamma$-rENaC, which normally produced only small amiloride-sensitive Na^+ conductance, generated a whole cell conductance that was indistinguishable to that obtained for wt $\alpha\beta\gamma$-rENaC (Fig. 5C). These effects were not observed when scrambled RNAi was injected. The contribution of Nedd4-2 to CK2 regulation of ENaC was further examined in mammalian cells. M1 cells were grown on permeable supports after treatment with RNAi for mCK2, mNedd4-2, or scrambled RNAi, or as nontransfected control cells (Fig. 5D). Knockdown of CK2 and Nedd4-2 was verified by Western blotting (supplemental Fig. S1). $I_{sc\text{-amil}}$ was enhanced in M1 cells following Nedd4-2 knockdown, and inhibition by TBB was largely reduced (Fig. 5D). In contrast, CK2 knockdown reduced $I_{sc\text{-amil}}$ and also abolished the effect of TBB on $I_{sc\text{-amil}}$ (Fig. 5D). Taken together, these results suggest that CK2 phosphorylation of ENaC antagonizes the inhibitory effects of Nedd4-2.

CK2 Controls Membrane Expression of β-ENaC and γ-ENaC— The activity of epithelial Na^+ channels largely depends on co-expression of both β- and γ-subunits. Membrane expression of β-ENaC and γ-ENaC was monitored by injecting $\alpha\beta_{Flag}\gamma$-ENaC or $\alpha\beta\gamma_{Flag}$-ENaC, respectively, and Na^+ conductances were measured in parallel. Na^+ conductances generated by either $\alpha\beta_{Flag}\gamma$-ENaC or $\alpha\beta\gamma_{Flag}$-ENaC, respectively, were almost completely abolished when oocytes were exposed to 10 μM TBB, while membrane expression of β_{Flag} and γ_{Flag} were reduced by about 50% (Fig. 6A). We further examined whether β_{Flag} and γ_{Flag} behave in a similar fashion in the absence of α-ENaC. Dimeric channels formed by $\beta_{Flag}\gamma$-ENaC or $\beta\gamma_{Flag}$-ENaC produced small but detectable amiloride-sensitive whole cell conductances (0.74 $\pm$ 0.2 μS; $n = 8$ and 0.2 $\pm$ 0.1 μS; $n = 7$, respectively). Interestingly expression of β_{Flag}-ENaC and γ_{Flag}-ENaC in dimeric and trimeric channels was similar, but expression of both subunits in the dimeric channel was not affected by TBB (data not shown). This suggests a complex role of α-ENaC for expression of $\beta\gamma$-ENaC.

To further assess the impact of CK2 phosphorylation on membrane expression of β-ENaC and γ-ENaC in trimeric ($\alpha\beta_{Flag}\gamma$-ENaC and $\alpha\beta\gamma_{Flag}$-ENaC) channels, we expressed single mutants ($\alpha\beta_{S631A\text{-}Flag}\gamma$-ENaC or $\alpha\beta\gamma_{T599A\text{-}Flag}$-ENaC) and double mutants ($\alpha\beta_{S631A\text{-}Flag}\gamma_{T599A}$-ENaC or $\alpha\beta_{S631A}\gamma_{T599A\text{-}Flag}$-ENaC) in the absence or presence of 10 μM TBB. For all mutant combinations, Na^+ conductances were largely reduced in comparison to that of wt-ENaC, and residual conductances generated by the double mutants were insensitive to TBB (Fig. 6, B and C). In contrast, the membrane expression of β-ENaC and γ-ENaC was not affected by any of the mutations individually, and membrane expression of the double mutants ($\alpha\beta_{S631A\text{-}Flag}\gamma_{T599A}$-ENaC; $\alpha\beta_{S631A}\gamma_{T599A\text{-}Flag}$-ENaC) was no longer inhibited by TBB (Fig. 6, B and C). These data suggest that when CK2 sites are present in β-ENaC and γ-ENaC, they need to be phosphorylated to allow proper membrane expression of all three subunits.

ENaC Translocates CK2 to the Cell Membrane— It has been reported that CK2 binds directly to ENaC (21). This suggests that CK2 may be translocated by ENaC to the cell membrane as found for CFTR (24). Oocytes expressing ENaC and non-injected control oocytes were immunolabeled, after embedding
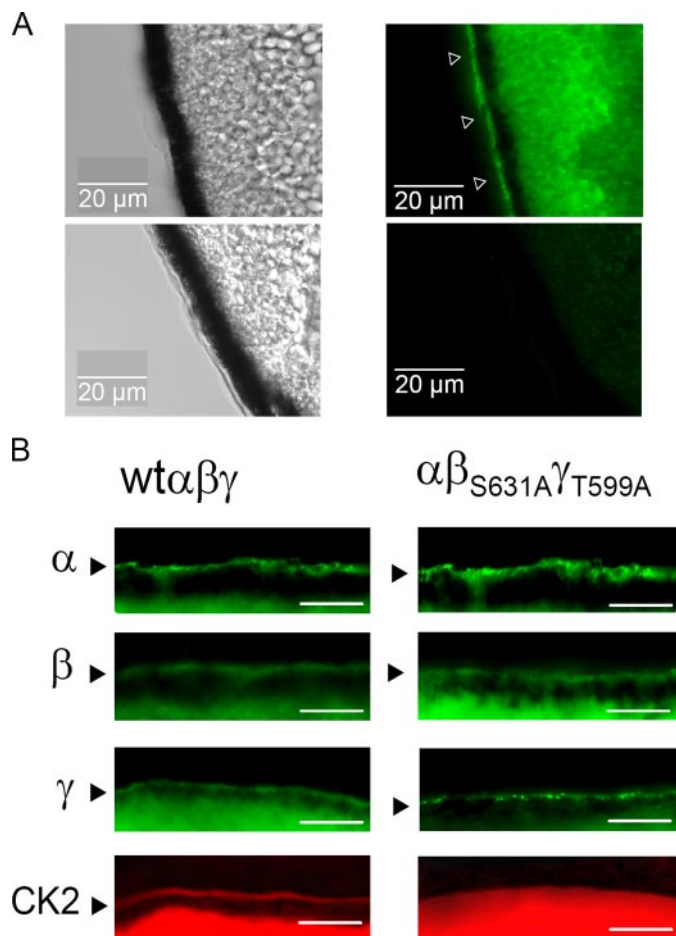
and cutting into 20-μm sections. Using an anti-FLAG antibody, α-ENaC could be visualized in membranes of *Xenopus* oocytes expressing $\alpha_{Flag}\beta\gamma$-ENaC (Fig. 7A). Moreover, upon expression of $\alpha\beta_{Flag}\gamma$-ENaC or $\alpha\beta\gamma_{Flag}$-ENaC, β- and γ-subunits could be immunolabeled in the oocyte membrane (Fig. 7B, *left panels*). Expression of the three subunits was similar in $\alpha\beta_{S631A}\gamma_{T559A}$-ENaC-injected oocytes (Fig. 7B, *right panels*). However, while CK2 was detected in membranes of oocytes expressing wt-ENaC, no membrane staining of CK2 was detectable in $\alpha\beta_{S631A}\gamma_{T559A}$-ENaC-injected oocytes (Fig. 7B, *lower panels*). These results suggest that CK2 may be translocated to oocyte membranes by binding to ENaC β- and γ-subunits.

DISCUSSION

CK2 Regulates Ion Channels— CK2 is an essential, constitutively regulated multifunctional protein kinase whose functions are not fully understood (21). CK2 is believed to insert into protein complexes bringing its constitutive activity to many signaling complexes (p53, ion channels, actin capping at membranes, lipid flippases, etc). Notably, CK2 controls trafficking

FIGURE 6. CK2 is not essential for membrane expression of β-ENaC and γ-ENaC. *A*, inhibition of membrane expression of β_{Flag}-ENaC and γ_{Flag}-ENaC and G_{amil} by 10 μM TBB. *B* and *C*, TBB inhibited membrane expression of β_{Flag}-ENaC and γ_{Flag}-ENaC in single mutants ($\alpha\beta_{S631A}\gamma$, $\alpha\beta\gamma_{T559A}$), but not in double mutants ($\alpha\beta_{S631A}\gamma_{T559A}$). G_{amil} was largely reduced for all mutants, and G_{amil} produced by the double mutants was no longer inhibited by TBB. *Dashed lines* indicate membrane expression and G_{amil} of wt-ENaC. The *asterisk* (*) indicates a significant effect of TBB (paired *t*-tests, 6–12 experiments for each series).

FIGURE 7. **wt-ENaC translocates CK2 to the cell membrane.** *A*, DIC image of the oocyte membrane (*left panels*) and immunostaining of α_{Flag}-ENaC in an ENaC-expressing (*right upper panel*) and a non-injected (*right lower panel*) oocyte. *B*, immunostaining of the three ENaC subunits (*green*) and CK2 (*red*) in wt-ENaC (*left panel*) and $\alpha\beta_{S631A}\gamma_{T559A}$-ENaC (*right panel*)-expressing oocytes. *Bars* indicate 10 μm. Experiments were performed in at least triplicates.

and sorting of trans-Golgi proteins. CK2 affects a number of membrane channels and pumps, among them is polycystin-2 (PC2), a divalent cation-selective channel. CK2 was shown to maintain the Ca^{2+} sensitivity of PC2. Elimination of a CK2 site in PC2 reduced its Ca^{2+} sensitivity, without changing membrane expression (5). Others reported the importance of phosphorylation of PC2 by CK2, for proper ciliary localization of the channel (13). CK2 also phosphorylates three critical serine residues within nephrocystin, another ciliary protein. CK2 phosphorylation is essential for co-localization of nephrocystin with the sorting protein PACS-1 at the base of cilia. Inhibition of CK2 was shown to eliminate interaction of PACS-1 and nephrocystin and to induce defective nephrocystin targeting (19). CK2 may thus be relevant to the common autosomal form of polycystic kidney disease.

We found here that ENaC is regulated by CK2 in a related manner, *i.e.* CK2 regulates ENaC activity as well as membrane expression. Lack of CK2 phosphorylation appears to reduce Nedd4-2 binding to ENaC, thereby enhancing channel activity and membrane expression. Notably, phosphorylation of ENaC by ERK inhibits both channel activity and membrane expression, and both effects are mediated by Nedd4-2 binding to ENaC (10).

CK2 has also been described to influence other ion channels, namely by regulating the current amplitude of voltage-dependent Ca^{2+} channels (14), as well as the Ca^{2+}-dependent gating of small conductance Ca^{2+}-activated K^+ channels (4). SK channels are organized in multiprotein complexes together with CK2 and PP2A, located in the postsynaptic pole of cochlear outer hair cells (4). Furthermore, CK2 has recently been found to regulate CFTR, the chloride channel that is defective in cystic fibrosis and, as in this study, CK2 becomes membrane-associated with CFTR (24). Once again both CK2 and PP2A co-localize with different domains of CFTR (16, 24). Importantly, CK2 binding may be disease relevant because phenylalanine 508 (F508), the common missing residue in most patients with CF, is critical in promoting the interaction with CFTR. In both CFTR-expressing *Xenopus* oocytes and cell-attached mammalian cells, inhibition of CK2 induced prompt closure of CFTR in less than 80 s (24). However, direct phosphorylation of CFTR by CK2 at Ser-511 close to F508 has not been confirmed by radio-labeling cells and direct phosphopeptide mapping, and the exact mechanism remains unknown. Moreover, CFTR expression determines the cellular localization of CK2, which in turn could affect other membrane conductances such as amiloride-sensitive Na^+ absorption. It is interesting to note that the effect of CK2 is not stimulatory of the function of all proteins studied to date. Indeed, CK2 is inhibitory of another ABC family member, ABCA1; thus, constitutively suppressing the lipid flippase activity of this CFTR-related protein.

C Terminus of β-ENaC, a Target for Kinase Regulation of ENaC—Phosphorylation-dependent regulation of ENaC by CK2 is demonstrated in the present study by several agents, namely, heparin, a nonspecific inhibitor of CK2 directed against acidic motifs; the peptide inhibitor of CK2; poly(E:Y); and the specific CK2 inhibitors TBB and DMAT. Inhibition of protein phosphatases with okadaic acid further increased Na^+ conductance, indicating the importance of basal CK2-dependent phosphorylation for ENaC regulation (3). Furthermore, elimination of CK2 phosphorylation sites (Ser-6331) abrogated Na^+ conductance in *Xenopus* oocytes. Thus, together with results obtained in native epithelia and in epithelial cells, these data show that ENaC is compellingly regulated by CK2 (Fig. 8). Notably, CK1 was shown recently to control intracellular trafficking of ENaC (25). Yet, in a previous report such regulation could not be detected in salivary duct cells (9). Instead, activation of ENaC by the G protein-coupled receptor kinase 2 Grk2 was found. Because of phosphorylation of Ser-633 by Grk2 in the C terminus of β-ENaC, the affinity of Nedd4-2 binding to ENaC is apparently reduced, thus enhancing ENaC currents. According to the present data (Fig. 5B), a similar scenario may hold true for CK2-dependent regulation of ENaC, because both phosphorylation sites for Grk2 and CK2 are located in close proximity to one other. Because CK2 classically engages in hierarchical phosphorylation with other kinases, phosphorylation through either Grk2 or CK2 could control EnaC activity and membrane expression depending on the cell type and expression levels of the kinases involved. Moreover, phosphorylation by CK2 is likely to affect regulation by Grk2 and *vice versa* (Fig. 5B). Further experiments will be needed to unravel this complex regulatory network and should focus on the inhibitory
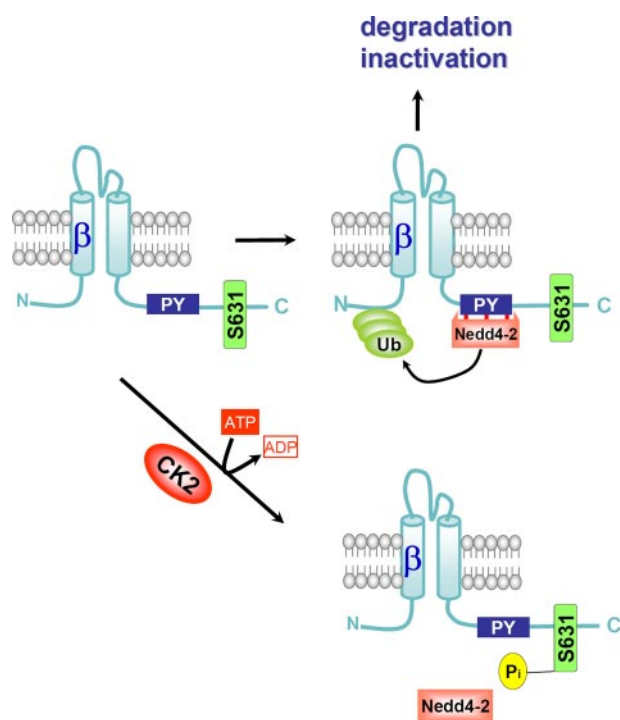
FIGURE 8. **Model for CK2 action on ENaC.** Binding of the ubiquitin ligase Nedd4-2 leads to ubiquitination of ENaC and subsequent degradation of the channel and/or channel inactivation. Phosphorylation of ENaC at Ser-631 reduces affinity of ENaC for Nedd4-2, thereby maintaining membrane localization and ENaC activity.

phosphorylation by Erk and its counteraction by activation through PKA, Grk2, and CK2, with Nedd4-2 as the central control switch (1, 9, 20, 26). As suggested in a previous report and supported by the present data, acute and chronic regulation may be different, inasmuch as acute regulation is changing the open probability of the channel, while chronic regulation by Nedd4-2 controls membrane expression (10).

REFERENCES

1. Awayda, M. S., Ismailov, I. I., Berdiev, B. K., Fuller, C. M., and Benos, D. J. (1996) *J. Gen. Physiol.* **108,** 49–65
2. Bachhuber, T., König, J., Voelcker, T., Mürle, B., Schreiber, R., and Kunzelmann, K. (2005) *J. Biol. Chem.* **280,** 31587–31594
3. Becchetti, A., Malik, B., Yue, G., Duchatelle, P., Al Khalili, O., Kleyman, T. R., and Eaton, D. C. (2002) *Am. J. Physiol. Renal Physiol.* **283,** F1030–F1045
4. Bildl, W., Strassmaier, T., Thurm, H., Andersen, J., Eble, S., Oliver, D., Knipper, M., Mann, M., Schulte, U., Adelman, J. P., and Fakler, B. (2004) *Neuron* **43,** 847–858
5. Cai, Y., Anyatonwu, G., Okuhara, D., Lee, K. B., Yu, Z., Onoe, T., Mei, C. L., Qian, Q., Geng, L., Wiztgall, R., Ehrlich, B. E., and Somlo, S. (2004) *J. Biol. Chem.* **279,** 19987–19995
6. Canessa, C. M., Schild, L., Buell, G., Thorens, B., Gautschl, I., Horisberger, J. D., and Rossier, B. C. (1994) *Nature* **367,** 463–467
7. Debonneville, C., Flores, S. Y., Kamynina, E., Plant, P. J., Tauxe, C., Thomas, M. A., Munster, C., Chraibi, A., Pratt, J. H., Horisberger, J. D., Pearce, D., Loffing, J., and Staub, O. (2001) *EMBO J.* **20,** 7052–7059
8. Diakov, A., and Korbmacher, C. (2004). *J. Biol. Chem.* **279,** 38134–38142
9. Dinudom, A., Fotia, A. B., Lefkowitz, R. J., Young, J. A., Kumar, S., and Cook, D. I. (2004) *Proc. Natl. Acad. Sci. U. S. A.* **101,** 11886–11890
10. Falin, R. A., and Cotton, C. U. (2007) *J. Gen. Physiol.* **130,** 313–328
11. Feldman, R. D. (2002) *Mol. Pharmacol.* **61,** 707–709
12. Firsov, D., Schild, L., Gautschi, I., Merillat, A. M., Schneeberger, E., and Rossier, B. C. (1996) *Proc. Natl. Acad. Sci. U. S. A.* **93,** 15370–15375
13. Hu, J., Bae, Y. K., Knobel, K. M., and Barr, M. M. (2006) *Mol. Biol. Cell* **17,** 2200–2211
14. Kimura, T., and Kubo, T. (2003) *Neurosci. Res.* **46,** 105–117
15. Kunzelmann, K., Schreiber, R., Nitschke, R., and Mall, M. (2000) *Pflügers Arch.* **440,** 193–201
16. Meggio, F., Boldyreff, B., Issinger, O. G., and Pinna, L. A. (1994) *Biochemistry* **33,** 4336–4342
17. Michlig, S., Harris, M., Loffing, J., Rossier, B. C., and Firsov, D. (2005) *J. Biol. Chem.* **280,** 38264–38270
18. Rajamanickam, J., Palmada, M., Lang, F., and Boehmer, C. (2007) *J. Neurochem.* **102,** 858–866
19. Schermer, B., Hopker, K., Omran, H., Ghenoiu, C., Fliegauf, M., Fekete, A., Horvath, J., Kottgen, M., Hackl, M., Zschiedrich, S., Huber, T. B., Kramer-Zucker, A., Zentgraf, H., Blaukat, A., Walz, G., and Benzing, T. (2005) *EMBO J.* **24,** 4415–4424
20. Shi, H., Asher, C., Chigaev, A., Yung, Y., Reuveny, E., Seger, R., and Garty, H. (2002) *J. Biol. Chem.* **277,** 13539–13547
21. Shi, H., Asher, C., Yung, Y., Kligman, L., Reuveny, E., Seger, R., and Garty, H. (2002) *Eur. J. Biochem.* **269,** 4551–4558
22. Snyder, P. M., Olson, D. R., Kabra, R., Zhou, R., and Steines, J. C. (2004) *J. Biol. Chem.* **279,** 45753–45758
23. Snyder, P. M., Olson, D. R., and Thomas, B. C. (2002) *J. Biol. Chem.* **277,** 5–8
24. Treharne, K. J., Crawford, R. M., Best, O. G., Schulte, E. A., Chen, J.-H., Gruenert, D. C., Wilson, S. M., Kunzelmann, K., Sheppard, D. N., and Mehta, A. (2007) *J. Biol. Chem.* **282,** 10804–10813
25. Yan, W., Spruce, L., Rosenblatt, M. M., Kleyman, T. R., and Rubenstein, R. C. (2007) *Am. J. Physiol. Renal Physiol.* **293,** F868–F876
26. Yang, L. M., Rinke, R., and Korbmacher, C. (2006) *J. Biol. Chem.* **281,** 9859–9868